The Journal of Experimental Medicine

Inflammatory monocytes recruited after skeletal muscle injury switch into antiinflammatory macrophages to support myogenesis

Ludovic Arnold,[1] Adeline Henry,[2] Françoise Poron,[1] Yasmine Baba-Amer,[1] Nico van Rooijen,[3] Anne Plonquet,[4] Romain K. Gherardi,[1] and Bénédicte Chazaud[1]

[1]Institut National de la Santé et de la Recherche Médicale, Unité 841, Institut Mondor de Recherche Biomédicale, "Cell Interactions in the Neuromuscular System" Team, Université Paris 12 Val-de-Marne, 94000 Créteil, France
[2]Plateforme Cytométrie Institut Mondor de Medecine Moleculaire, IFR10, Université Paris 12 Val-de-Marne, 94000 Créteil, France
[3]Vrije Universiteit, Vrije Universiteit Medisch Centrum, Department of Molecular Cell Biology, Faculty of Medicine, 1081 BT Amsterdam, Netherlands
[4]Assistance Publique-Hôpitaux de Paris, Groupe Henri Mondor-Albert Chenevier, Service d'immunologie-Biologie, 94000 Créteil, France

Macrophages (MPs) are important for skeletal muscle regeneration in vivo and may exert beneficial effects on myogenic cell growth through mitogenic and antiapoptotic activities in vitro. However, MPs are highly versatile and may exert various, and even opposite, functions depending on their activation state. We studied monocyte (MO)/MP phenotypes and functions during skeletal muscle repair. Selective labeling of circulating MOs by latex beads in CX3CR1$^{GFP/+}$ mice showed that injured muscle recruited only CX3CR1^{lo}/Ly-6C^{+} MOs from blood that exhibited a nondividing, F4/80^{lo}, proinflammatory profile. Then, within muscle, these cells switched their phenotype to become proliferating antiinflammatory CX3CR1^{hi}/Ly-6C^{-} cells that further differentiated into F4/80^{hi} MPs. In vitro, phagocytosis of muscle cell debris induced a switch of proinflammatory MPs toward an antiinflammatory phenotype releasing transforming growth factor β1. In co-cultures, inflammatory MPs stimulated myogenic cell proliferation, whereas antiinflammatory MPs exhibited differentiating activity, assessed by both myogenin expression and fusion into myotubes. Finally, depletion of circulating MOs in CD11b-diphtheria toxin receptor mice at the time of injury totally prevented muscle regeneration, whereas depletion of intramuscular F4/80^{hi} MPs at later stages reduced the diameter of regenerating fibers. In conclusion, injured skeletal muscle recruits MOs exhibiting inflammatory profiles that operate phagocytosis and rapidly convert to antiinflammatory MPs that stimulate myogenesis and fiber growth.

CORRESPONDENCE
Bénédicte Chazaud:
benedicte.chazaud@creteil.inserm.fr

Abbreviations used: CCR, CC chemokine receptor; clo-lip, clodronate-encapsulated liposome; DEX, dexamethasone; DT, diphtheria toxin; DTR, DT receptor; LX, latex bead; MO, monocyte; MP, macrophage; mpc, myogenic precursor cell; PPAR, peroxisome proliferator-activated receptor; SLPI, secretory leukocyte protease inhibitor; TA, tibialis anterior.

Stromal cells are involved in organogenic processes by controlling parenchymal cell functions such as migration, proliferation, differentiation, and programmed cell death (1). Among stromal cells, macrophages (MPs) play a major role in the maintenance of tissue homeostasis (2). In addition to phagocytosis and antigen presentation, these cells play a supportive function in various tissues (2, 3). However, MPs are renowned for their heterogeneity, as reflected by the various specialized functions they adopt in different anatomical locations (2, 4). Many of these activities appear to be opposing in nature (e.g., proinflammatory vs. antiinflammatory, immunogenic vs. tolerogenic, and tissue-destructive vs. tissue-repair activities) (4).

Different activation states have been described in vitro for MPs, each being associated with a particular phenotype and function (2, 5). Classical activation, obtained after LPS/IFN-γ treatment, induces production of proinflammatory cytokines and reactive oxygen species. Alternative activation, obtained after IL-4 treatment, increases expression of the mannose receptor (CD206). Deactivation by IL-10 and glucocorticoids induces production of IL-10, TGF-β1, and expression of the scavenger receptor CD163. However, it is not known to what extent these distinct activation states exist in vivo and whether MP fate is determined forever or whether it remains constantly malleable (2), although several in vitro studies have shown MP adaptation to a changing microenvironment (4, 6–8).

An additional degree of complexity is reached with the existence of several subsets of circulating monocytes (MOs). In both the human and mouse, two main MO subsets are present in blood: the main CD14^{hi} CD16^{-} (CX3CR1^{lo}/Ly-6C^{hi} in the mouse) MO subset that invades tissues during acute inflammation and the CD14^{lo} CD16^{+} (CX3CR1^{hi}/Ly-6C^{lo} in the mouse) MO subset, which is not (or to a lesser extent) recruited during inflammation (9–13) but is expanded in chronic diseases such as HIV infection, sepsis, tuberculosis, or asthma (14). Both fate and function of this population remain unclear, because in mouse, it is present in the normal spleen and may correspond to MPs residing in normal tissues (9). However, there is growing evidence that they may result from the maturation of Ly-6C^{hi} MOs (11, 15, 16).

MPs are involved in skeletal muscle repair. Muscle damage induces massive MP infiltration at the injury site (17, 18). Partial depletion of MOs/MPs impairs muscle regeneration, whereas reconstitution of bone marrow restores regeneration (19–23). Initially limited to phagocytosis of necrotic fibers, the proregenerative role of MPs has been shown to involve a direct stromal support function (24, 25). We have previously shown that MO-derived MPs enhance myogenic cell growth (26). MPs release mitogenic growth factors for myogenic precursor cells (mpcs) and establish cell–cell interactions that protect mpcs from apoptosis (26, 27). However, little is known about both MO/MP subsets and phenotypes at work during muscle regeneration. Studies in the rat have shown that ED1^{+} MPs are associated with muscle necrosis, whereas ED2^{+} (CD163) MPs, regarded as "resident MPs," invade muscle

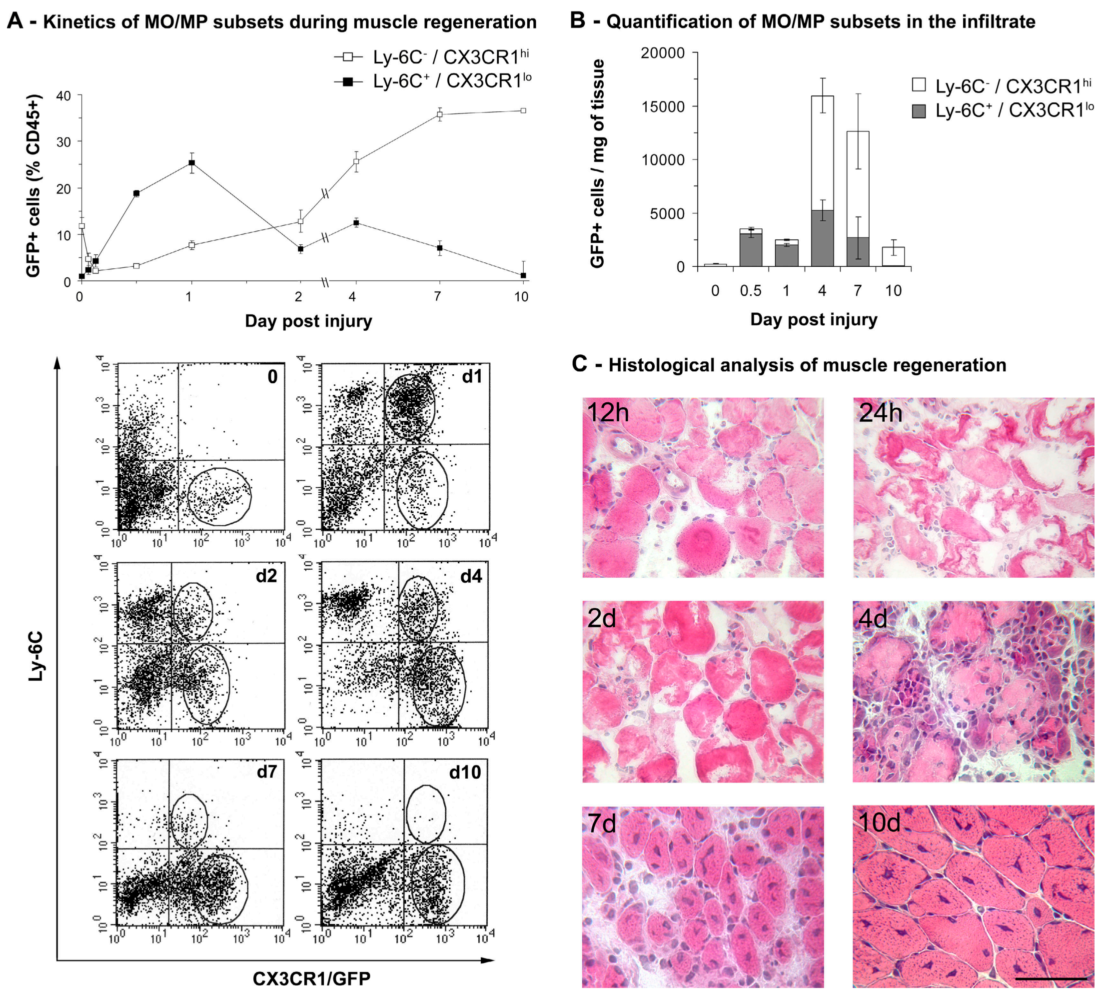

Figure 1. Kinetics of MO/MP subsets during muscle regeneration in the CX3CR1$^{GFP/+}$ mouse. (A) CD45^{+} cells present in injured muscle were analyzed for Ly-6C and GFP (CX3CR1) expression by flow cytometry. (top) Results are expressed as the percentage of CD45^{+} cells isolated from muscle and represent the means ± SD of three experiments. (bottom) Representative examples of FACS analysis at each time point. The two circles represent the two gated MO populations. (B) Total number of MOs/MPs was calculated from results obtained in A, and the number of isolated CD45^{+} cells were plotted to muscle weight. Results represent the means ± SD of three experiments. (C) Representative hematoxylin and eosin staining of muscle sections at various times after notexin injection. Bar, 50 μm.

once necrosis has been removed and are associated with regenerative myofibers (17, 28). Although the nature of ED1 and ED2 MPs is not characterized, these results suggest that different MP subpopulations are associated with different stages of muscle repair.

In this study, we used in vivo tracing methods to analyze which MO subset was recruited after muscle injury, ex vivo phenotyping analyses to characterize the MO/MP profile during muscle regeneration, in vitro co-culture experiments to identify which MP phenotype was associated with myogenesis, and sequential in vivo MO/MP depletion studies to evaluate the respective roles of both circulating and i.m. MOs/MPs in skeletal muscle repair.

RESULTS

Two MO/MP subsets are sequentially present during muscle regeneration

MOs/MPs collected from skeletal muscle of the CX3CR1$^{GFP/+}$ mouse (9, 15) were analyzed according to their GFP and Ly-6C expression during muscle regeneration. Normal muscle contained little CX3CR1^{hi}/Ly-6C^{-} MOs/MPs (~200 cells/mg of muscle). Notexin was injected in tibialis anterior (TA) muscles to induce the necrosis/regeneration process. As soon as 90 min after injury, CX3CR1^{lo}/Ly-6C^{+} MOs/MPs were detected in muscle and rapidly invaded the tissue to reach a maximum point at 24 h after injury (25% of CD45^{+} cells). The CX3CR1^{lo}/Ly-6C^{+} MO/MP population quickly declined with time, whereas the CX3CR1^{hi}/Ly-6C^{-} MOs/MPs appeared and continuously increased to reach a plateau at day 7 accounting for 35% of CD45^{+} cells extracted from muscle at this time point (Fig. 1 A).

The MO/MP percentage among CD45^{+} cells is a relative quantification that does not reflect the amount of MOs/MPs actually present in muscle. Thus, we calculated from these data the total number of extracted GFP^{+} cells per milligram of muscle. Results indicated that the extent of the two MO/MP waves was different (Fig. 1 B), and this was confirmed by histological examination (Fig. 1 C). During the first 2 d, as injured myofibers became necrotic, 2,000 to 3,500 GFP^{+} cells/mg of muscle were counted. At 4 and 7 d, when myogenic cells proliferated and further differentiated (Fig. 1 C), five- to sixfold more GFP^{+} MOs/MPs were found in muscle (12,000–16,000 cells/mg; Fig. 1 B). 10 d after injury, when centrally nucleated fibers were visible throughout the injured area (Fig. 1 C), the amount of GFP^{+} cells had dramatically declined to reach <2,000 GFP^{+} cells/mg of tissue (Fig. 1 B).

CX3CR1^{lo}/Ly-6C^{+} and CX3CR1^{hi}/Ly-6C^{-} MO/MP populations display distinct proliferative and inflammatory profiles

Between days 1 and 4 after injury, the number of Ly-6C^{-} MOs/MPs increased 20-fold, while the number of Ly-6C^{+} MOs/MPs increased twofold (Fig. 1 B). We analyzed proliferation of both subsets that were isolated from regenerating muscle by cell sorting (Fig. 2 A). Ki67 labeling showed that Ly-6C^{+} MOs/MPs never proliferated, whereas Ly-6C^{-} MOs/MPs partially entered into cell cycle from day 2, and the number of proliferating cells doubled at day 4 and further decreased by twofold at day 7 (Fig. 2 B).

To examine the inflammatory profile of the two MO/MP populations, we analyzed cytokine expression of isolated Ly-6C^{-} and Ly-6C^{+} MOs/MPs at day 4 after injury by RT-PCR. Results showed that Ly-6C^{+} MOs/MPs expressed IL-1β and, to a lesser extent, TNF-α transcripts more strongly than Ly-6C^{-} MOs/MPs (Fig. 2 C). Conversely, Ly-6C^{-} MOs/MPs expressed TGF-β1 and IL-10 more strongly than Ly-6C^{+} MOs/MPs (Fig. 2 C), indicating that Ly-6C^{+} MOs/MPs had an inflammatory profile and Ly-6C^{-} MOs/MPs had an antiinflammatory profile.

Injured muscle only recruits CX3CR1^{lo}/Ly-6C^{+} MOs/MPs that subsequently switch into antiinflammatory CX3CR1^{hi}/Ly-6C^{-} MOs/MPs and differentiate into MPs

We labeled each circulating subset with fluorescent latex beads (LXs) before injury, as previously described (12, 15). Labeling of MOs does not alter their migratory capacities (12). After i.v.

A - Sorting of MO/MP subsets

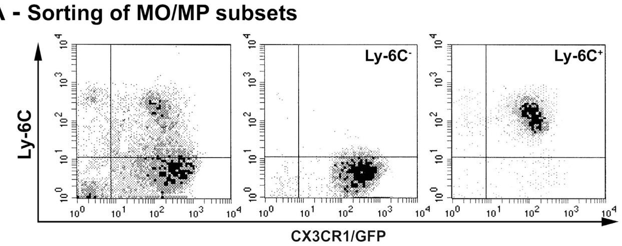

B - Ki67 labeling of Ly-6C+ and Ly-6C- MO/MP subsets

h/d post injury	15h	48h	4d	7d
CX3CR1^{hi} Ly-6C^{-}	0 ± 0	13.5 ± 2.9	27 ± 4.9	12.8 ± 4.9
CX3CR1^{lo} Ly-6C^{+}	0 ± 0	0 ± 0	0 ± 0	0 ± 0

C - Cytokine expression of Ly-6C+ and Ly-6C- MO/MP subsets

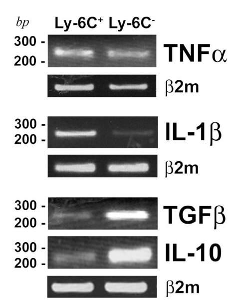

band intensity

	Ly-6C^{+}	Ly-6C^{-}
TNFα	100	82
IL-1β	100	60
TGFβ	100	193
IL-10	100	230

Figure 2. Phenotype of Ly-6C^{+} and Ly-6C^{-} MOs/MPs during muscle regeneration. Ly-6C^{+} and Ly-6C^{-} MO/MP subsets were isolated by cell sorting at various times after injury. (A) Representative example of cell sorting of Ly-6C^{-} (middle) and Ly-6C^{+} (right) cells from whole MOs/MPs (left) at day 4 after injury. (B) Ki67 immunostaining is expressed as the percentage of isolated MOs/MPs. (C) Expression of TNF-α, IL-1β, TGF-β1, and IL-10 was analyzed by RT-PCR in isolated populations at day 4 after injury. Corresponding band intensities are given as the means of three experiments.

LX injection, circulating LX$^+$ cells were CX3CR1^{hi}/Ly-6C$^-$ MOs (Fig. 3 A, top, blood); LX$^+$ cells were never detected in muscle after injury (Fig. 3 A, top, muscle), indicating that Ly-6C$^-$ MOs/MPs appearing in muscle at day 2 were not recruited from blood. After clodronate-encapsulated liposome (clo-lip) injection followed by LX injection, circulating LX$^+$ cells were CX3CR1^{lo}/Ly-6C$^+$ MOs, as previously described (15). 36 h after notexin injection, LX$^+$ cells were still Ly-6C$^+$ MOs (95%) in the blood (Fig. 3 A, bottom, blood), while LX$^+$ cells present within muscle were both Ly-6C$^+$ and Ly-6C$^-$ (38 ± 2 and 61 ± 3%, respectively, based on three experiments; Fig. 3 A, bottom right, muscle). These data indicate that muscle Ly-6C$^-$ cells derived from early recruited Ly-6C$^+$ MOs/MPs.

Several markers have been associated with MP phenotype transition at the time of resolution of inflammation. Among them, secretory leukocyte protease inhibitor (SLPI) is induced in MPs by proinflammatory signals to trigger down-regulation of proinflammatory cues (29–32). RT-PCR analysis showed that Ly-6C$^+$ MOs/MPs strongly expressed SLPI compared with Ly-6C$^-$ MOs/MPs (62% increase of band intensity based on three experiments; Fig. 3 B) 4 d after injury. Inversely, peroxisome proliferator-activated receptor (PPAR) γ is expressed by MPs that down-regulate inflammation (33–35). Our results showed that PPAR-γ mRNA was strongly expressed by Ly-6C$^-$ compared with Ly-6C$^+$ MOs/MPs (49% increase of band intensity based on three experiments; Fig. 3 B).

Forward and side scatter of the two MO/MP subsets isolated at day 7 after injury showed that Ly-6C$^-$ MOs/MPs had higher side scatter and were larger than Ly-6C$^+$ MOs/MPs (Fig. 3 C), in accordance with a maturation of the Ly-6C$^-$ subset. Analysis of differentiation markers showed that Ly-6C$^-$ MOs/MPs expressed CD11c and higher levels of F4/80 (Fig. 3 C). Nearly all (> 90%) F4/80$^+$ cells were CD11c$^+$ and I-A^{b+}, and no positivity was observed for the dendritic cell marker DEC-205 (unpublished data). These results show that, contrary to Ly-6C$^+$ MOs/MPs, Ly-6C$^-$ MOs/MPs exhibited high levels of MP differentiation markers.

Collectively, these results suggest that after muscle injury, inflammatory Ly-6C$^+$ MOs are recruited from blood, convert to antiinflammatory Ly-6C$^-$ MOs/MPs that proliferate in situ, and further differentiate into mature MPs.

Phagocytosis of muscle cell debris participates in MP phenotype transition

To study interactions between MPs and myogenic cells possibly involved in MP phenotype transition, we used in vitro human cell co-cultures. Indeed, in vitro pro- and antiinflammatory MP activation states described in humans most likely correspond to Ly-6C$^+$ and Ly-6C$^-$ MO/MP profiles found in regenerating mouse muscle. Consistently, LPS/IFN-γ treatment of human MPs induced TNF-α ($P < 0.05$) and IL-1β ($P < 0.05$) secretion (Fig. 4 A), whereas dexamethasone (DEX)/IL-10 treatment induced IL-10 ($P < 0.05$) secretion (Fig. 4 A), as previously shown (36, 37). Because differentiating muscle cells secrete IL-4 (38), a key inducer of alternative activation of MPs (5), we tested IL-4 treatment,

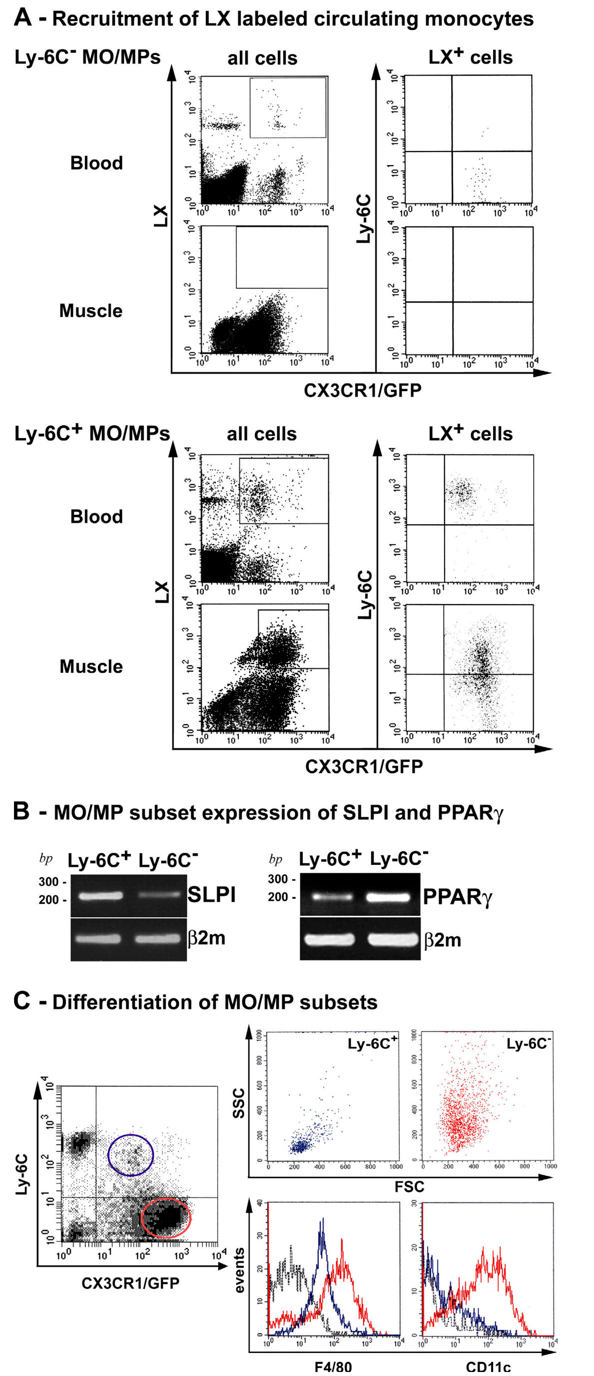

Figure 3. Fate of Ly-6C$^+$ and Ly-6C$^-$ MOs/MPs during muscle regeneration. (A) Circulating Ly-6C$^-$ (top) and Ly-6C$^+$ (bottom) MOs were labeled with LX red microspheres and analyzed by flow cytometry. LX$^+$ CD45$^+$ GFP$^+$ cells (gates in all cells; left) were analyzed for Ly-6C expression (LX$^+$ cells; right) in both blood and muscle at day 3 (for Ly-6C$^-$ labeling) and day 2 (for Ly-6C$^+$ labeling) after injury. Results are representative of three experiments. (B) SLPI and PPAR-γ expression was analyzed by RT-PCR in Ly-6C$^+$ and Ly-6C$^-$ MOs/MPs sorted at day 4 after injury. (C) Flow cytometry analysis of forward scatter (FSC)/side scatter (SSC) characteristics, F4/80 and CD11c expression of Ly-6C$^+$ (blue), and Ly-6C$^-$ (red) MOs/MPs sorted at day 7 after injury (black dotted line, isotypic control). Results are representative of three experiments.

which induced TGF-β1 secretion (Fig. 4 A), as previously shown (39).

As a major role of MPs is to operate phagocytosis of dead cells, we evaluated the effect of phagocytosis of muscle cell debris on the MP inflammatory profile. Upon phagocytosis of necrotic mpcs, LPS/IFN-γ–treated MPs both decreased their TNF-α secretion ($P < 0.05$) and increased their TGF-β1 secretion ($P < 0.03$; Fig. 4 B). We attempted to inhibit phagocytosis of proinflammatory MPs by colchicine (40), cytochalasin D (41), and recombinant Annexin V (42). Colchicine failed to inhibit phagocytosis, and MPs changed their cytokine secretion upon mpc debris phagocytosis, as in untreated cells (Fig. 4 C). Conversely, phagocytosis was inhibited in the presence of cytochalasin D or recombinant Annexin V; in these conditions, TNF-α and TGF-β1 secretion did not change in the presence of mpc debris (Fig. 4 C). These data indicate that phagocytosis of mpc debris induced a switch of the MP phenotype toward an antiinflammatory profile, as previously shown for other cell types (43–46).

We also evaluated whether interactions with living mpcs may influence MP phenotype. Neither addition of mpcs to previously activated MPs nor addition of mpcs before MP activation substantially altered the MP phenotype (unpublished data). These data show that mpcs neither modified the MP activation state nor prevented acquisition of any given MP phenotype.

Inflammatory MPs increase mpc growth, whereas antiinflammatory MPs stimulate their differentiation

In co-culture experiments, we analyzed mpc behavior depending on MP activation state. We have previously shown that untreated MPs stimulate mpc growth and proliferation (26). As shown in Fig. 5, mpc differentiation (Fig. 5 C) and fusion (Fig. 5 D) were also increased by untreated MPs ($P \leq 0.05$). LPS/IFN-γ–treated MPs were more potent in enhancing mpc growth (63%; $P < 0.05$; Fig. 5 A), and accordingly, they enhanced mpc proliferation, as shown by increased BrdU incorporation (25%; $P < 0.05$; Fig. 5 B). Inversely, both myogenin expression (Fig. 5 C) and myotube formation (Fig. 5 D) were strongly reduced (58 and 68%, respectively; $P < 0.05$), indicating an inhibition of differentiation by inflammatory MPs. IL-4–treated MPs slightly reduced mpc proliferation (14%; $P < 0.05$; Fig. 5 B), whereas they stimulated myogenin expression (28%; $P < 0.05$; Fig. 5 C) and stimulated myotube formation (158%; $P < 0.05$; Fig. 5 D) compared with untreated MPs. DEX/IL-10–treated MPs did not stimulate growth (Fig. 5 A) and proliferation (Fig. 5 B) compared with untreated MPs but presented a strong prodifferentiating activity, as assessed by increased myogenin expression (52%; $P < 0.05$; Fig. 5 C) and increased myotube formation (136%; $P < 0.01$; Fig. 5 D). These results strongly suggest that the activation state of MPs may monitor the myogenic process.

MO/MP presence is mandatory for skeletal muscle regeneration

We took advantage of the CD11b–diphtheria toxin receptor (DTR) mouse to study the respective roles of MO/MP subsets during muscle regeneration in vivo, because i.m. injection of clo-lip is toxic for myogenic cells (unpublished data). In CD11b-DTR mice, MOs (and possibly tissue MPs, depending on the way of injection) are depleted after DT injection (47). After a single i.v. DT injection, circulating MO loss occurred from 6 h and reached a maximum

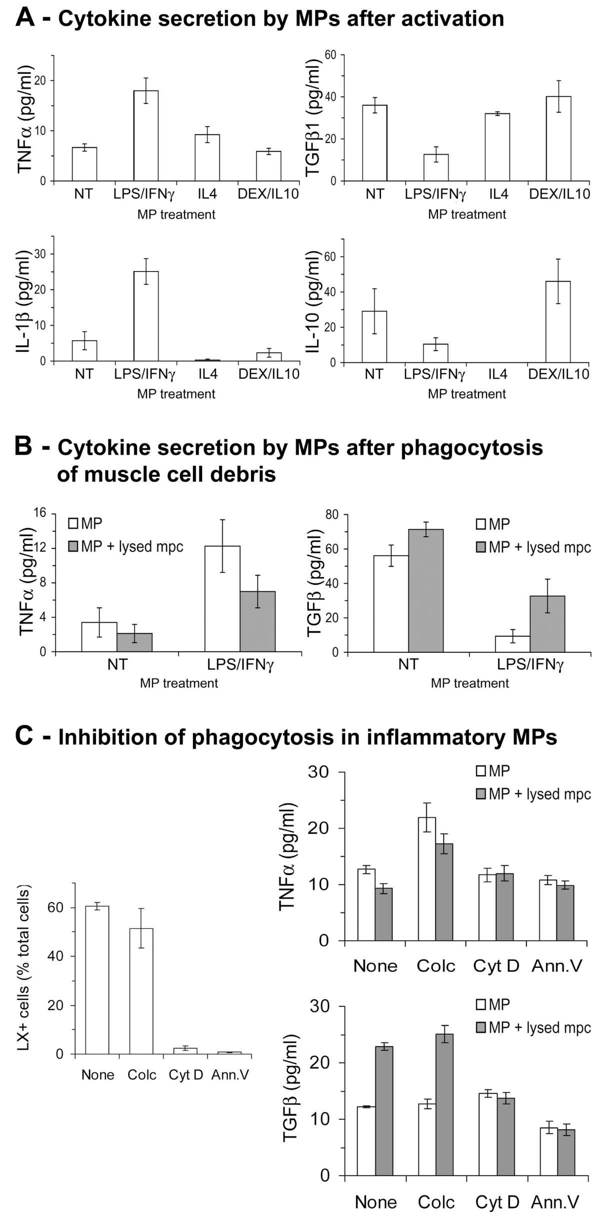

Figure 4. Phagocytosis and cytokine secretion by activated MPs. Cytokine secretion was evaluated by ELISA in MP-conditioned medium. (A) Cytokine secretion by untreated (NT) and LPS/IFN-γ–, IL-4–, and DEX/IL-10–treated MPs. (B) Cytokine secretion by untreated (NT) and LPS/IFN-γ–treated MPs after phagocytosis of muscle cell debris. (C, left) Phagocytosis of LXs by LPS/IFN-γ–treated MPs incubated or not (none) with colchicine (colc), cytochalasin D (cyt D), or recombinant Annexin V (Ann.V). (right) Cytokine secretion by LPS/IFN-γ–treated MPs after phagocytosis of muscle cell debris in the presence of the same effectors. Results represent the means ± SEM of three experiments.

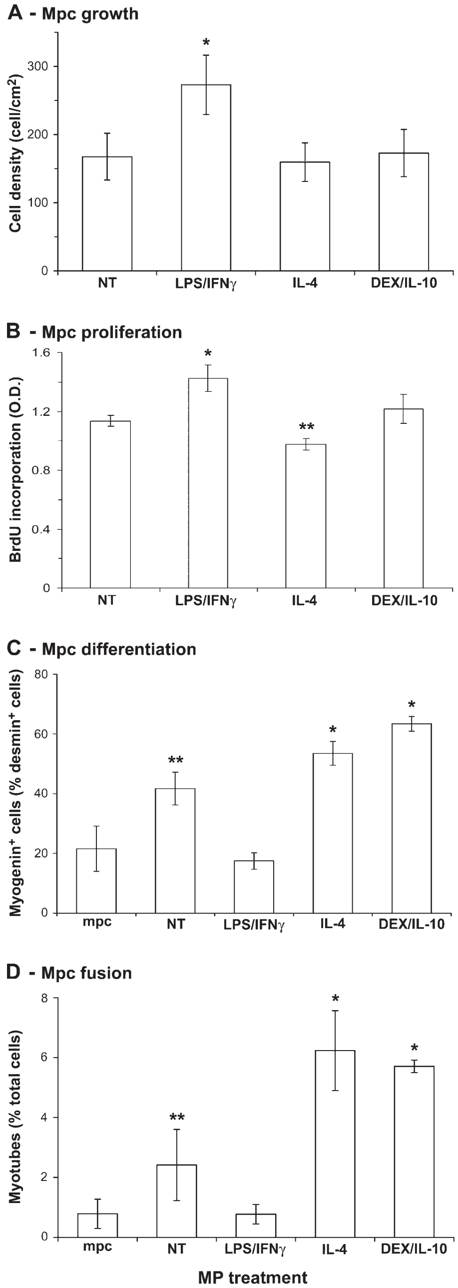

Figure 5. Effects of activated MPs on mpc fate. mpcs were co-cultured with untreated (NT) and LPS/IFN-γ–, IL-4–, and DEX/IL-10–treated MPs and further analyzed for their (A) growth, (B) proliferation, (C) differentiation, and (D) fusion. All parameters were analyzed at day 3 of co-culture except for BrdU incorporation, which was monitored during 24 h of co-culture. Results represent the means ± SEM of three experiments. Asterisks above bars indicate significant differences ($P < 0.05$).

at 12 h, which lasted 12 h longer, with subsequent restoration and normalization at 48 h (Fig. 6 A). At maximum depletion, 75–80% of cells in the MO gate had disappeared (Fig. 6 A), as did F4/80$^+$, CD11b$^+$, and Ly6C$^+$ cells (not depicted). The time course of postinjury muscle regeneration in untreated CD11b-DTR mice was similar to that of the C57BL/6 mouse shown in Fig. 1 until day 4, but centrally nucleated myofibers appeared earlier in CD11b-DTR than in C57BL/6 mice (day 7 vs. 10; Fig. 6 B). When DT was simultaneously injected at (Fig. 6 C) or 12 h before (Fig. 6 D) muscle injury, necrotic fibers were removed more slowly, and regeneration was impaired with the appearance of adipose cells (Fig. 6, C and D; and Fig. 7). After double DT injection, both 12 h before and simultaneously at notexin injection (which induced a MO depletion lasting 0–24 h after injury), almost no MO/MP infiltration was observed (Fig. 6 E). None of the hallmarks of regeneration were detected, and persistence of necrotic fibers was observed until day 7 (Fig. 6 E and Fig. 7), although circulating MOs reappeared in the circulation from day 2 after injury (not depicted). When DT was injected 4 d after notexin, no difference was observed compared with the control (Fig. 6 B and Fig. 7), indicating that circulating MOs were no longer recruited into muscle at this time. Notably, i.v.-injected DT did not notably affect i.m. MOs/MPs, as shown by unchanged expression of both F4/80 and CD11b by CD45$^+$ cells isolated from muscle (Fig. 6 F, inset).

We attempted to target i.m. antiinflammatory MOs/MPs at a time when phagocytosis of necrotic myofibers is finished (Fig. 6 B and Fig. 7 A). To assess MP depletion in muscle, flow cytometric analysis of CD45$^+$ cells was performed 24 h after a single i.m. DT injection. The total number of F4/80$^+$ cells present in muscle was diminished by 25% after DT injection (especially F4/80^{hi} cells, which were diminished by 75%; $P < 0.05$; Fig. 8 A), indicating that these differentiated FSC^{hi}F4/80^{hi} MPs, corresponding to Ly-6C$^-$ MPs, were targeted by DT. However, the total number of CD45$^+$ cells increased by twofold in DT- versus PBS-injected muscle (Fig. 8 A), indicating that i.m. DT injection induced a secondary inflammation accompanied by the recruitment of F4/80$^-$ leukocytes (likely neutrophiles and F4/80$^{lo/-}$ MOs). Consistently, histological examination of whole TA muscle 4–5 d later showed an area in which new cycles of regeneration were visible, as assessed by the presence of necrotic and basophilic fibers (Fig. 8 B, arrow). This area was restricted to the site of needle puncture and was therefore excluded from the analysis to avoid counting of small regenerating myofibers coming from the secondary lesion (Fig. 8 B). The diameter of centrally nucleated regenerating myofibers was evaluated in the rest of the TA and was found to be reduced by 41% in DT- versus PBS-injected muscle (30.8 vs. 18.2 μm, respectively; $P < 0.001$; Fig. 8 C).

DISCUSSION

In the present study, we have shown that (a) injured skeletal muscle selectively recruits Ly-6C$^+$ circulating MOs that exhibit an inflammatory profile; (b) within muscle, Ly-6C$^+$ MOs switch their phenotype to acquire an antiinflammatory profile, with phagocytosis of muscle cell debris being most likely involved in this transition; (c) as necrosis disappears from the injured area, antiinflammatory Ly-6C$^-$ MOs/MPs proliferate and further differentiate into MPs; (d) in vitro, inflammatory MPs enhance myogenic cell proliferation and repress their differentiation, whereas antiinflammatory MPs

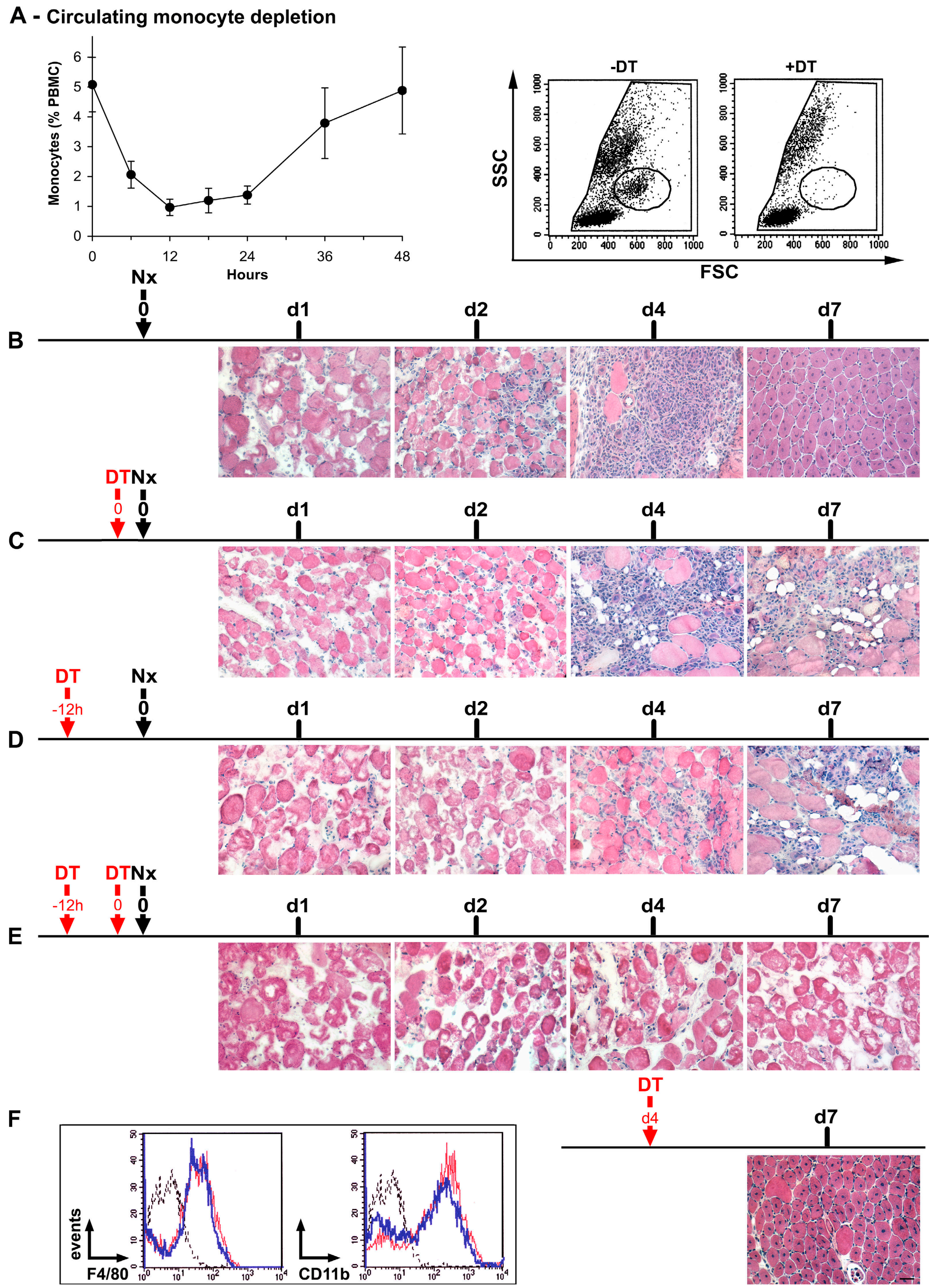

Figure 6. Effects of circulating MO depletion on skeletal muscle regeneration. (A, left) Kinetics of circulating MO depletion after one i.v. DT injection. Results represent the means ± SD of at least four experiments. (right) Examples of FACS analysis of blood before (−DT) and 18 h after i.v. DT injection (+DT). Circles show MO gate. (B–F) Notexin (Nx) was injected into the TA of CD11b-DTR mice at day 0, and DT was injected i.v. at various times, as indicated by the red arrows. Muscle histology was analyzed until day 7 after hematoxylin and eosin staining. Results are representative of at least two independent experiments. (F, inset) CD45+ cells were isolated from muscle and analyzed for F4/80 and CD11b expression 24 h after an i.v. DT (blue line) or PBS (red line) injection at day 4 after injury (black dotted line, isotypic control). Bar, 50 μm.

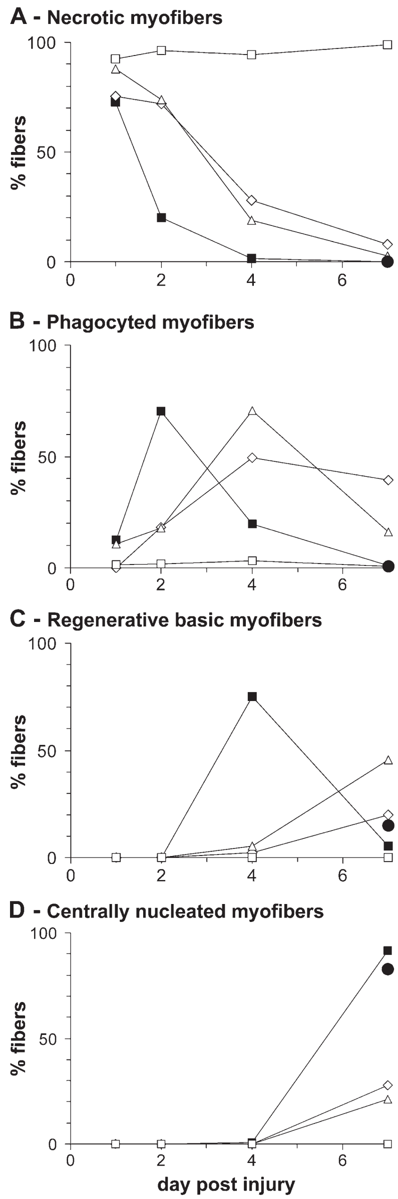

Figure 7. Quantitative analysis of muscle regeneration after circulating MO depletion. CD11b-DTR mice were treated as in Fig. 6, and in each case the number of (A) necrotic myofibers, (B) phagocyted myofibers, (C) regenerating basic myofibers, and (D) centrally nucleated regenerating myofibers was evaluated. Closed squares represent the control corresponding to Fig. 6 B; open diamonds represent simultaneous DT and notexin injections corresponding to Fig. 6 C; open triangles represent a DT injection 12 h before notexin injection corresponding to Fig. 6 D; open squares represent a double DT injection corresponding to Fig. 6 E; and closed circles represent a DT injection 4 d after notexin injection corresponding to Fig. 6 F. Results are expressed as the percentage of total counted myofibers and are the means of at least two experiments.

stimulate myogenesis and fusion; and (e) in vivo depletion of circulating MOs at the time of injury totally prevents muscle regeneration, whereas later depletion of i.m. MPs decreases the diameter of regenerating fibers.

It has been shown that the CX3CR1^{lo}/Ly-6C^{+} MO population is recruited in injured or inflamed tissues (9, 13, 48). Our experiments using LX-labeled circulating MOs showed that CX3CR1^{lo}/Ly-6C^{+} MOs were selectively recruited rapidly after muscle injury. Mouse CX3CR1^{lo}/Ly-6C^{+} MOs and their human analogues bear several chemokine receptors, including CC chemokine receptor (CCR) 2, CCR1, CCR4, CCR7, CXC chemokine receptor 1, and CXC chemokine receptor 2 (9). The corresponding chemokines are expressed by muscle tissue during the first days after injury (the cytokine expression profile is available at http://pepr.cnmcresearch.org) (22, 49, 50). Monocyte chemoattractant protein–1 has been particularly involved in MO recruitment by injured muscle (19, 20). We did not evidence recruitment of CX3CR1^{hi}/Ly-6C^{-} MOs from blood to muscle. Moreover, transient depletion of circulating MOs during the first 0–24 h after muscle injury showed no subsequent MP infiltration despite reconstitution of the pool of circulating MOs. This suggests that CX3CR1^{lo}/Ly-6C^{+} MO/MP recruitment takes place early after injury (i.e., within 2–3 d after injury).

Our experiments showed that initially LX-labeled CX3CR1^{lo}/Ly-6C^{+} MOs converted to CX3CR1^{hi}/Ly-6C^{-} MOs/MPs from day 2 after injury, indicating a phenotype transition of MOs/MPs within muscle. Consistently, MP differentiation markers were weakly expressed by CX3CR1^{lo}/Ly-6C^{+} MOs/MPs and markedly expressed by CX3CR1^{hi}/Ly-6C^{-} MOs/MPs (see below). We propose that CX3CR1^{lo}/Ly-6C^{+} cells, which exhibit an inflammatory phenotype (expressing TNF-α and IL-1β), progressively lose Ly-6C expression while converting to antiinflammatory MOs/MPs (expressing TGF-β1 and IL- 10). These data are in accordance with the cytokine mRNA analysis of postinjured muscle extract (available at http://pepr.cnmcresearch.org) (51): TNF-α and IL-1β expression peaks at days 2–3 after injury, whereas IL-10 and TGF-β1 expression increases from day 2 after injury and is maintained throughout regeneration. MP phenotype conversion observed in skeletal muscle further supports previous in vitro evidence that MPs are capable of rapid adaptation to changing environments (4, 6–8) and in vivo demonstration that MPs alter their phenotype according to their tissue environment (52).

MPs participate in both amplification of inflammation at the time of injury and down-regulation of the inflammatory response to avoid excess tissue damage (31, 53, 54). MP stop signals associated with the resolution of inflammation include induction of negative regulators of inflammation in MPs by environmental cues and nonphlogistic phagocytosis. As shown herein, both likely operate during skeletal muscle regeneration. SLPI is considered as a brake on the response of MPs to inflammation (29, 31). Its expression is induced by LPS and IL-6 and leads to inhibition of NO and TNF-α production (30). In vivo, the highest SLPI synthesis occurs during the proinflammatory phase and, thus, anticipates an increase in TGF-β1 and IL-10 production (32). Accordingly, we have shown that CX3CR1^{lo}/Ly-6C^{+} MOs/MPs expressed more SLPI than CX3CR1^{hi}/Ly-6C^{-} cells. Another marker associated with the resolution of inflammation by

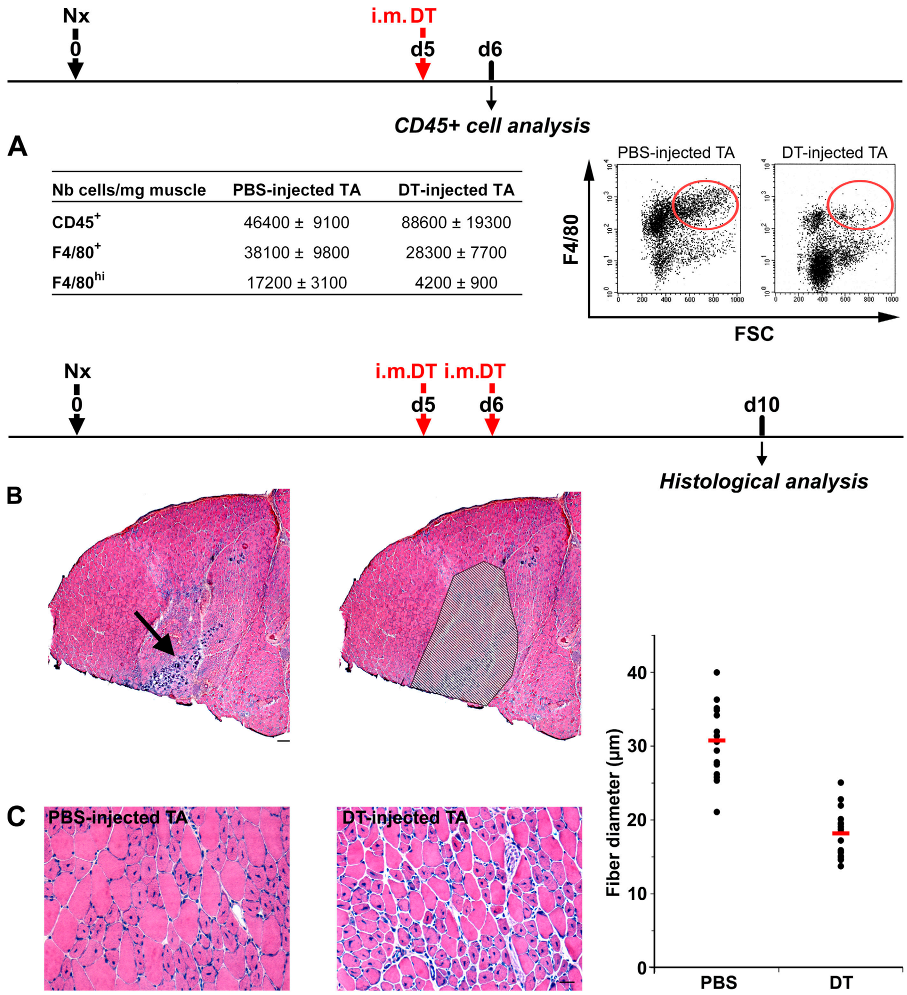

Nb cells/mg muscle	PBS-injected TA	DT-injected TA
$CD45^+$	46400 ± 9100	88600 ± 19300
$F4/80^+$	38100 ± 9800	28300 ± 7700
$F4/80^{hi}$	17200 ± 3100	4200 ± 900

Figure 8. Effects of i.m. DT injection on skeletal muscle regeneration. Notexin (Nx) was injected into the TA of CD11b-DTR mice at day 0, and DT was injected in the same muscle at day 5 (A) and days 5 and 6 (B and C). (A) 24 h after a single i.m. DT injection, $CD45^+$ cells were isolated from muscle and analyzed for F4/80 expression. Red circles enclose $FSC^{hi}/F4/80^{hi}$ cells. (B) Reconstituted whole view of TA muscle at day 10 after Notexin injection (hematoxylin and eosin staining), presenting hallmarks of secondary regeneration restricted to the site of needle puncture (arrow). (right) Hatched area represents the area excluded from analysis. Bar, 200 μm. (C) PBS- and DT-injected muscles were analyzed at day 10 after injury for myofiber diameter evaluation (hematoxylin and eosin staining). Quantified results are given for three independent experiments, with each point corresponding to a field (red bars represent the means). Bar, 50 μm.

MPs is PPAR-γ. Fatty acids and prostaglandin metabolites bind to PPAR-γ in activated MPs, which triggers inhibition of both inducible NO synthase and release of proinflammatory cytokines (33, 35), thus conferring antiinflammatory properties to PPAR-γ (34). In this paper, we showed that antiinflammatory $CX3CR1^{hi}/Ly\text{-}6C^-$ MOs/MPs strongly expressed PPAR-γ. Nonphlogistic phagocytosis by MPs is another signal for switching to healing (31). Binding and phagocytosis of apoptotic cells inhibit secretion of proinflammatory mediators and stimulate secretion of TGF-β1 and IL-10 by inflammatory MPs (43–46). Induction of an antiinflammatory process by phagocytosis of necrotic cells depends on the cell type ingested (42, 43, 55). We showed that both unstimulated and inflammatory MPs adopted an antiinflammatory profile upon phagocytosis of necrotic muscle cell debris and that inhibition of MP phagocytosis prevented this phenotype switch. Collectively, these results strongly suggest that recruited inflammatory $CX3CR1^{lo}/Ly\text{-}6C^+$ MOs/MPs convert to antiinflammatory $CX3CR1^{hi}/Ly\text{-}6C^-$ MOs/MPs upon both ingestion of muscle cell debris and expression of stop signals extinguishing inflammation.

Our results showed that once switched, $CX3CR1^{hi}/Ly\text{-}6C^-$ MOs/MPs actively proliferated, therefore contributing to the large amounts of MOs/MPs observed in muscle at days 4–7 after injury. In vitro, MP proliferation is inhibited by inflammatory mediators (LPS, IFN-γ, NO, and IL-6) and is stimulated by TGF-β1 (56–58). Thus, proliferation of recruited MOs/MPs may be caused by changes in their environment, although as yet unknown mechanisms related to the change of phenotype cannot be excluded. Later during muscle regeneration (day 7), $CX3CR1^{hi}/Ly\text{-}6C^-$ MO/MP proliferation slowed down simultaneously with the complete differentiation into MPs, as shown by their strong F4/80 expression (59). Almost all F4/80$^+$ cells were also positive for CD11c and MHCII, as previously observed after inflammation in various organs (60, 61), and were DEC-205$^-$. In the blood, Ly-6C$^-$ MOs, which come from Ly-6C$^+$ cells, are also CD11c$^+$ (12). Therefore, the appearance of CD11c$^+$ cells in the muscle may be a recapitulation of conversion from Ly-6C$^+$/CD11c$^-$ to Ly-6C$^-$/CD11c$^+$ MOs within the tissue. Thus, proliferating CX3CR1^{hi}/Ly-6C$^-$ MOs/MPs and differentiating CX3CR1^{hi}/Ly-6C$^-$ MPs are associated with the regenerative phase of muscle repair.

Depending on the context, MPs may have supportive or deleterious effects on cells: in chronic diseases, including those affecting skeletal muscle, MPs are deleterious (62, 63), whereas they support tissue repair in muscle and other various tissues, including the liver, brain, peripheral nerve, and epithelium (19–22, 64–67). With the exception of regulation of inflammation, studies documenting a direct role of MPs on cell behavior are scant and include intestinal progenitor proliferation (65), erythroblast proliferation and maturation (68), and oligodendrocytic differentiation and myelination (69). In vitro studies have shown that the MP activation state may direct neural progenitor differentiation toward either neurogenesis or oligodendrogenesis (70). Our results substantiate the view that MP function may be related to an activation state. In coculture experiments, inflammatory MPs (the counterpart of inflammatory CX3CR1^{lo}/Ly-6C$^+$ cells observed in vivo) stimulated mpc proliferation and inhibited their differentiation. Inversely, IL-4 treated and antiinflammatory MPs exhibited a strong differentiating activity on mpcs, assessed by both stimulation of myogenic program and increase of fusion into multinucleated cells. Molecular mechanisms involved in these processes are currently under investigation. It is likely that cytokines released by activated MPs influence myogenic cell behavior: TNF-α is mitogenic for myoblasts and inhibits their differentiation (71, 72), IL-1β impairs myogenic differentiation through insulin-like growth factor–1 (73), and in vitro effects of TGF-β1 are more controversial, although in vivo neutralization of TGF-β1 in regenerating muscle was shown to reduce the diameter of regenerating myofibers (74). Beyond cytokines, cyclooxygenase 2 and its metabolites may also play a role, as they were shown to be fusogenic and necessary for good muscle repair (75–77).

Previous in vivo studies using different injury models have shown that partial reduction of MO/MP entry into injured muscle hinders muscle regeneration, as shown by a delay in the appearance of regenerating myofibers and the persistence of intermuscular adipocytes (19–22). We observed similar features upon partial inhibition of MO recruitment in toxic-induced muscle regeneration. Moreover, when nearly no MO/MP was allowed to enter damaged muscle, myofibers remained in the necrotic state, indicating the indispensable role of MPs in muscle repair. Interestingly, despite the normalized level of circulating MOs from day 2 after injury, no delayed recruitment was observed, suggesting that signals governing MO recruitment are only transiently expressed by the damaged tissue, as was recently documented in ultraviolet-injured skin (48). Accordingly, depletion of circulating MOs at day 4 after injury had no effect on muscle regeneration. On the other hand, depletion of i.m. antiinflammatory F4/80^{hi} MOs/MPs at the time of regeneration (i.e., once phagocytosis of necrotic myofibers is achieved) reduced the diameter of the centrally nucleated regenerating myofibers, indicating that these MOs/MPs were involved in fiber growth, in accordance with our in vitro data.

In conclusion, our data demonstrate a phenotype transition operated by recruited MOs/MPs during resolution of inflammation and tissue repair, which is associated with changes in their functions. We propose sequential involvements of these two phenotypically distinct MP populations during skeletal muscle repair as follows: within the first 24–48 h after injury, skeletal muscle recruits inflammatory circulating MOs, which stimulate myogenic cell proliferation and prevent their differentiation. While they are exposed to an inflammatory environment and operate phagocytosis of muscle cell debris, inflammatory MOs/MPs convert to antiinflammatory MOs/MPs. As phagocytosis of necrotic myofibers is finished, these antiinflammatory MOs/MPs actively proliferate and further differentiate into antiinflammatory MPs that sustain myogenic differentiation and myofiber growth in addition to their protective effect on differentiating myotubes (27) and their effect on fiber membrane repair (78).

MATERIALS AND METHODS

Animals. C57BL/6, CX3CR1$^{gfp/+}$ (9), and CD11b-DTR (provided by J.S. Duffield, Harvard Medical School, Boston, MA) (47) mice were bred and used according to French legislation. Experiments were conducted at 4–8 wk of age.

Muscle injury and muscle preparation. 10 µl notexin (25 µg/ml in PBS; Latoxan) was injected in the TA. For histological analysis, muscles were prepared as previously described (27). Quantitative analysis of muscle regeneration was performed on the entire injured area: approximately seven fields (20× objective; PL Flustar; Carl Zeiss MicroImaging, Inc.) were analyzed in each mouse, representing 300–400 fibers per mouse. Myofiber diameter was evaluated after collagen IV immunolabeling (see Immunolabeling) on approximately seven fields (20× objective) in each mouse. The small diameter of only centrally nucleated myofibers was evaluated in late-regenerating muscle (nonhatched area in Fig. 8 B) with Axiovision 4.6 software (Carl Zeiss MicroImaging, Inc.), representing 250–350 fibers per mouse. In PBS-injected mice, the punctured fascicule was omitted from analysis.

Isolation of MOs/MPs from muscle. Fascia of the TA was removed. Muscles were dissociated in DMEM containing collagenase B 0.2% (Roche Diagnostics GmbH) and trypsine-EDTA 0.2% at 37°C for 45 min twice, filtered, and counted. CD45+ cells were isolated using magnetic sorting (Miltenyi Biotec) and stained with PE- or PC5-conjugated anti-Gr1 antibody (which reacts with Ly-6C and Ly-6G, but only Ly-6C is expressed by MOs; eBioscience). Cells were sorted using a cell sorter (Epics Elite; Beckman Coulter). Populations presenting >90% purity were used. In some experiments, PE-conjugated CD11c, I-A^b (BD Biosciences) and F4/80 (AbD Serotec) antibodies were used. Analysis was performed with a cytometer (FACSCalibur; BD Biosciences).

Labeling of blood MOs. Labeling of circulating MOs was performed exactly as previously described (15) with plain microspheres (Fluoresbrite Polychromatic Red Microspheres 0.5µm, 2.5% solids; PolySciences, Inc.) and clo-lip, which were prepared as previously described (79). Clodronate was a gift of Roche Diagnostics GmbH.

Depletion of circulating MOs and i.m. MPs. 12 ng/g DT was i.v. injected into CD11b-DTR mice. Blood was retroorbitally harvested at various times after injection, and cells were labeled with anti-CD11b, anti-Gr1, and F4/80 antibody and analyzed by flow cytometry. Because of high interindividual variations (3–12% of PBMCs), the number of circulating MOs in control mice was normalized to 5% of PBMCs for each series (mean calculated with >25 mice). To deplete infiltrated MOs/MPs, 25 ng/g DT in <10 μl was i.m. injected at days 5 and 6 after injury. Controls included injection of PBS.

Immunolabeling. Muscle slides were incubated with anticollagen IV antibody (1:50; Chemicon International, Inc.) revealed with Cy5-conjugated anti–rabbit antibody. Mouse-sorted cells were centrifugated on slides and labeled with 1 μg/ml anti-Ki67 antibody (Abcam plc), revealed with FITC-conjugated anti–rabbit antibody. Cultured human mpcs were incubated with 60 μg/ml antidesmin antibody (Abcam plc), revealed by a Cy3-conjugated anti–rabbit antibody, and with 10 μg/ml antimyogenin antibody (BD Biosciences), revealed by a biotinylated anti–mouse (Vector Laboratories) and by dichlororotriazinglaminofluorescein-streptavidin (Beckman Coulter). Controls included incubation with whole rabbit or mouse IgGs. Other secondary antibodies and IgGs were obtained from Jackson ImmunoResearch Laboratories.

RT-PCR. Total RNA was prepared from sorted cells using the RNeasy mini kit (QIAGEN). 0.5 μg of total RNA was reverse transcripted using Superscript II reverse transcriptase and amplified with a platinum Taq DNA polymerase (Invitrogen) and the following specific primers (sense and antisense, respectively): β2 microglobulin, 5′-CAGTTCCACCCGCCTCAC-3′ and 5′-CACATGTCTCGATCCCAG-3′; TNF-α, 5′-TTCCAGATTCTTC-CCTGAGGT-3′ and 5′-TAAGCAAAAGAGGAGGCAACA-3′; IL-1β, 5′-TGACGTTCCCATTAGACAACTG-3′ and 5′-CCGTCTTTCATTA-CACAGGACA-3′; TGF-β1, 5′-GAGACGGAATACAGGGCTTTC-3′ and 5′-TCTCTGTGGAGCTGAAGCAAT-3′; IL-10, 5′-ACCAGCTGGACA-ACATACTGC-3′ and 5′-TCACTCTTCACCTGCTCCACT-3′; SLPI, 5′-CCTTAAGCTTGAGAAGCCACA-3′ and 5′-AGCACTTGTATTTG-CCGTCAC; and PPAR-γ, 5′-AAGAGCTGACCCAATGGTTG-3′ and 5′-GGATCCGGCAGTTAAGATCA-3′. Amplification was performed at 94°C, 60°C, and 72°C for 1 min for each step for 30 cycles. 10 μl of amplification products was subjected to electrophoresis on a 2% agarose gel containing ethidium bromide for visualization. Quantification was performed by using Image software (Scion).

Human mpc culture. Culture media components were purchased from Invitrogen. Human mpcs were cultured from muscle samples at the time of corrective surgery, in conformity with French legislation (Code de la Santé Publique, livre II), as previously described (26).

Human MP cell culture. MPs were differentiated from MOs isolated from human blood, as previously described (26). Differentiated MPs were further cultured in either RPMI 1640 medium containing 15% FBS or advanced RPMI 1640 medium containing 0.5% FBS (supplemented with 1% sodium pyruvate, 10 mM Hepes, 50 μM β-mercaptoethanol, 1% nonessential amino acids, 100× 1% vitamins). MPs were treated, or not, for 48 h with either 1 μg/ml LPS (Sigma-Aldrich) and 10 ng/ml IFN-γ (PeproTech), or 10 ng/ml IL-4 (PeproTech) or 80 ng/ml DEX (Sigma-Aldrich) and 10 ng/ml IL-10 (PeproTech).

Phagocytosis. mpc necrosis was induced by H_2O treatment for 1 h at 37°C. 100% of cells were propidium iodide positive. Necrotic mpcs were seeded on MPs (five dead mpcs for one MP) for 3 h at 37°C. MP cultures were washed three times to remove noningested material and further cultured in serum-free advanced RPMI 1640 supplemented medium over 24 h to make conditioned media. In some experiments, cells were treated, as previously described, with 10 μg/ml colchicine (Sigma-Aldrich) (40), 1 μg/ml cytochalasin D (Sigma-Aldrich) (41), or 40 μg/ml recombinant Annexin V (BD Biosciences) (42). Phagocytosis was quantified in the same conditions after incubation with fluorescent microspheres (as described in Labeling of blood MOs). The number of LX^+ cells was quantified under an inverted microscope and expressed as the percentage of total cells.

Co-cultures. mpcs were plated on previously prepared MP cultures (3:1 MP/mpc ratio) in advanced RPMI 1640 supplemented medium, except in some experiments in which MPs and mpcs were seeded together before MP treatment was applied, as described in Human MP cell culture.

mpc behavior. mpc growth was evaluated as previously described (26). mpc proliferation was estimated by BrdU incorporation (Roche Diagnostics GmbH). mpc differentiation was evaluated by counting the number of myogenin$^+$ cells among desmin$^+$ cells. mpc fusion was estimated by counting the number of nuclei per myotube.

Statistical analyses. All experiments were performed using at least three different cultures or animals in independent experiments. The Student's *t* test was used for statistical analyses. $P < 0.05$ was considered significant.

We wish to thank J.S. Duffield for the gift of CD11b-DTR mice, G.J. Randolph for advice on circulating MO labeling, F.J. Authier and P. Lafuste for helpful discussions, and E. Fernandez and M. Balbo for technical assistance.

This work was supported by Association Française contre les Myopathies, the Institut National de la Santé et de la Recherche Médicale, and the Université Paris 12 Val-de-Marne.

The authors have no conflicting financial interests.

Submitted: 8 January 2007
Accepted: 21 March 2007

REFERENCES

1. Lapidot, T., and I. Petit. 2002. Current understanding of stem cell mobilization: the roles of chemokines, proteolytic enzymes, adhesion molecules, cytokines, and stromal cells. *Exp. Hematol.* 30:973–981.
2. Gordon, S., and P.R. Taylor. 2005. Monocyte and macrophage heterogeneity. *Nat. Rev. Immunol.* 5:953–964.
3. Gordon, S. 1995. The macrophage. *Bioessays.* 17:977–986.
4. Stout, R.D., and J. Suttles. 2004. Functional plasticity of macrophages: reversible adaptation to changing microenvironments. *J. Leukoc. Biol.* 76:509–513.
5. Gordon, S. 2003. Alternative activation of macrophages. *Nat. Rev. Immunol.* 3:23–35.
6. Gratchev, A., J. Kzhyshkowska, K. Kothe, I. Muller-Molinet, S. Kannookadan, J. Utikal, and S. Goerdt. 2006. Mphi1 and Mphi2 can be re-polarized by Th2 or Th1 cytokines, respectively, and respond to exogenous danger signals. *Immunobiology.* 211:473–486.
7. Porcheray, F., S. Viaud, A.C. Rimaniol, C. Leone, B. Samah, N. Dereuddre-Bosquet, D. Dormont, and G. Gras. 2005. Macrophage activation switching: an asset for the resolution of inflammation. *Clin. Exp. Immunol.* 142:481–489.
8. Stout, R.D., C. Jiang, B. Matta, I. Tietzel, S.K. Watkins, and J. Suttles. 2005. Macrophages sequentially change their functional phenotype in response to changes in microenvironmental influences. *J. Immunol.* 175:342–349.
9. Geissmann, F., S. Jung, and D.R. Littman. 2003. Blood monocytes consist of two principal subsets with distinct migratory properties. *Immunity.* 19:71–82.
10. Ancuta, P., L. Weiss, and N. Haeffner-Cavaillon. 2000. CD14+CD16++ cells derived in vitro from peripheral blood monocytes exhibit phenotypic and functional dendritic cell-like characteristics. *Eur. J. Immunol.* 30:1872–1883.
11. Sunderkotter, C., T. Nikolic, M.J. Dillon, N. van Rooijen, M. Stehling, D.A. Drevets, and P.J. Leenen. 2004. Subpopulations of mouse blood monocytes differ in maturation stage and inflammatory response. *J. Immunol.* 172:4410–4417.
12. Tacke, F., D. Alvarez, T.J. Kaplan, C. Jakubzick, R. Spanbroek, J. Llodra, A. Garin, J. Liu, M. Mack, N. van Rooijen, et al. 2007. Monocyte

subsets differentially employ CCR2, CCR5, and CX3CR1 to accumulate within atherosclerotic plaques. *J. Clin. Invest.* 117:185–194.
13. Swirski, F.K., P. Libby, E. Aikawa, P. Alcaide, F.W. Luscinskas, R. Weissleder, and M.J. Pittet. 2007. Ly-6Chi monocytes dominate hypercholesterolemia-associated monocytosis and give rise to macrophages in atheromata. *J. Clin. Invest.* 117:195–205.
14. Fingerle, G., A. Pforte, B. Passlick, M. Blumenstein, M. Strobel, and H.W. Ziegler-Heitbrock. 1993. The novel subset of CD14+/CD16+ blood monocytes is expanded in sepsis patients. *Blood.* 82:3170–3176.
15. Tacke, F., F. Ginhoux, C. Jakubzick, N. van Rooijen, M. Merad, and G.J. Randolph. 2006. Immature monocytes acquire antigens from other cells in the bone marrow and present them to T cells after maturing in the periphery. *J. Exp. Med.* 203:583–597.
16. Varol, C., L. Landsman, D.K. Fogg, L. Greenshtein, B. Gildor, R. Margalit, V. Kalchenko, F. Geissmann, and S. Jung. 2007. Monocytes give rise to mucosal, but not splenic, conventional dendritic cells. *J. Exp. Med.* 204:171–180.
17. McLennan, I.S. 1996. Degenerating and regenerating skeletal muscles contain several subpopulations of macrophages with distinct spatial and temporal distributions. *J. Anat.* 188:17–28.
18. Pimorady-Esfahani, A., M.D. Grounds, and P.G. McMenamin. 1997. Macrophages and dendritic cells in normal and regenerating murine skeletal muscle. *Muscle Nerve.* 20:158–166.
19. Contreras-Shannon, V., O. Ochoa, S.M. Reyes-Reyna, D. Sun, J.E. Michalek, W.A. Kuziel, L.M. McManus, and P.K. Shireman. 2007. Fat accumulation with altered inflammation and regeneration in skeletal muscle of CCR2 −/− mice following ischemic injury. *Am. J. Physiol. Cell Physiol.* 292:C953–C967.
20. Shireman, P.K., V. Contreras-Shannon, O. Ochoa, B.P. Karia, J.E. Michalek, and L.M. McManus. 2006. MCP-1 deficiency causes altered inflammation with impaired skeletal muscle regeneration. *J. Leukoc. Biol.* 81:775–785; 10.1189/jlb.0506356.
21. Summan, M., G.L. Warren, R.R. Mercer, R. Chapman, T. Hulderman, N. van Rooijen, and P.P. Simeonova. 2006. Macrophages and skeletal muscle regeneration: a clodronate-containing liposome depletion study. *Am. J. Physiol. Regul. Integr. Comp. Physiol.* 290:R1488–R1495.
22. Warren, G.L., T. Hulderman, D. Mishra, X. Gao, L. Millecchia, L. O'Farrell, W.A. Kuziel, and P.P. Simeonova. 2004. Chemokine receptor CCR2 involvement in skeletal muscle regeneration. *FASEB J.* 19:413–415.
23. Grounds, M.D. 1987. Phagocytosis of necrotic muscle in muscle isografts is influenced by the strain, age, and sex of host mice. *J. Pathol.* 153:71–82.
24. Robertson, T.A., M.A.L. Maley, M.D. Grounds, and J.M. Papadimitriou. 1993. The role of macrophages in skeletal muscle regeneration with particular reference to chemotaxis. *Exp. Cell Res.* 207:321–331.
25. Cantini, M., and U. Carraro. 1995. Macrophage-released factor stimulates selectively myogenic cells in primary muscle culture. *J. Neuropathol. Exp. Neurol.* 54:121–128.
26. Chazaud, B., C. Sonnet, P. Lafuste, G. Bassez, A.C. Rimaniol, F. Poron, F.J. Authier, P.A. Dreyfus, and R.K. Gherardi. 2003. Satellite cells attract monocytes and use macrophages as a support to escape apoptosis and enhance muscle growth. *J. Cell Biol.* 163:1133–1143.
27. Sonnet, C., P. Lafuste, L. Arnold, M. Brigitte, F. Poron, F.J. Authier, F. Chretien, R.K. Gherardi, and B. Chazaud. 2006. Human macrophages rescue myoblasts and myotubes from apoptosis through a set of adhesion molecular systems. *J. Cell Sci.* 119:2497–2507.
28. St Pierre, B.A., and J.G. Tidball. 1994. Differential response of macrophage subpopulations to soleus muscle reloading after rat hindlimb suspension. *J. Appl. Physiol.* 77:290–297.
29. Jin, F., C.F. Nathan, D. Radzioch, and A. Ding. 1998. Lipopolysaccharide-related stimuli induce expression of the secretory leukocyte protease inhibitor, a macrophage-derived lipopolysaccharide inhibitor. *Infect. Immun.* 66:2447–2452.
30. Jin, F.Y., C. Nathan, D. Radzioch, and A. Ding. 1997. Secretory leukocyte protease inhibitor: a macrophage product induced by and antagonistic to bacterial lipopolysaccharide. *Cell.* 88:417–426.
31. Nathan, C. 2002. Points of control in inflammation. *Nature.* 420:846–852.
32. Odaka, C., T. Mizuochi, J. Yang, and A. Ding. 2003. Murine macrophages produce secretory leukocyte protease inhibitor during clearance of apoptotic cells: implications for resolution of the inflammatory response. *J. Immunol.* 171:1507–1514.
33. Ricote, M., A.C. Li, T.M. Willson, C.J. Kelly, and C.K. Glass. 1998. The peroxisome proliferator-activated receptor-gamma is a negative regulator of macrophage activation. *Nature.* 391:79–82.
34. Moore, K.J., M.L. Fitzgerald, and M.W. Freeman. 2001. Peroxisome proliferator-activated receptors in macrophage biology: friend or foe? *Curr. Opin. Lipidol.* 12:519–527.
35. Alleva, D.G., E.B. Johnson, F.M. Lio, S.A. Boehme, P.J. Conlon, and P.D. Crowe. 2002. Regulation of murine macrophage proinflammatory and anti-inflammatory cytokines by ligands for peroxisome proliferator-activated receptor-gamma: counter-regulatory activity by IFN-gamma. *J. Leukoc. Biol.* 71:677–685.
36. Hogger, P., J. Dreier, A. Droste, F. Buck, and C. Sorg. 1998. Identification of the integral membrane protein RM3/1 on human monocytes as a glucocorticoid-inducible member of the scavenger receptor cysteine-rich family (CD163). *J. Immunol.* 161:1883–1890.
37. Stein, M., S. Keshav, N. Harris, and S. Gordon. 1992. Interleukin 4 potently enhances murine macrophage mannose receptor activity: a marker of alternative immunologic macrophage activation. *J. Exp. Med.* 176:287–292.
38. Horsley, V., K.M. Jansen, S.T. Mills, and G.K. Pavlath. 2003. IL-4 acts as a myoblast recruitment factor during mammalian muscle growth. *Cell.* 113:483–494.
39. Song, E., N. Ouyang, M. Horbelt, B. Antus, M. Wang, and M.S. Exton. 2000. Influence of alternatively and classically activated macrophages on fibrogenic activities of human fibroblasts. *Cell. Immunol.* 204:19–28.
40. Lucas, M., L.M. Stuart, A. Zhang, K. Hodivala-Dilke, M. Febbraio, R. Silverstein, J. Savill, and A. Lacy-Hulbert. 2006. Requirements for apoptotic cell contact in regulation of macrophage responses. *J. Immunol.* 177:4047–4054.
41. Cvetanovic, M., and D.S. Ucker. 2004. Innate immune discrimination of apoptotic cells: repression of proinflammatory macrophage transcription is coupled directly to specific recognition. *J. Immunol.* 172:880–889.
42. Brouckaert, G., M. Kalai, D.V. Krysko, X. Saelens, D. Vercammen, M. Ndlovu, G. Haegeman, K. D'Herde, and P. Vandenabeele. 2004. Phagocytosis of necrotic cells by macrophages is phosphatidylserine dependent and does not induce inflammatory cytokine production. *Mol. Biol. Cell.* 15:1089–1100.
43. Fadok, V.A., D.L. Bratton, L. Guthrie, and P.M. Henson. 2001. Differential effects of apoptotic versus lysed cells on macrophage production of cytokines: role of proteases. *J. Immunol.* 166:6847–6854.
44. Huynh, M.L., V.A. Fadok, and P.M. Henson. 2002. Phosphatidylserine-dependent ingestion of apoptotic cells promotes TGF-beta1 secretion and the resolution of inflammation. *J. Clin. Invest.* 109:41–50.
45. Savill, J., and V. Fadok. 2000. Corpse clearance defines the meaning of cell death. *Nature.* 407:784–788.
46. Xu, W., A. Roos, N. Schlagwein, A.M. Woltman, M.R. Daha, and C. van Kooten. 2006. IL-10-producing macrophages preferentially clear early apoptotic cells. *Blood.* 107:4930–4937.
47. Duffield, J.S., S.J. Forbes, C.M. Constandinou, S. Clay, M. Partolina, S. Vuthoori, S. Wu, R. Lang, and J.P. Iredale. 2005. Selective depletion of macrophages reveals distinct, opposing roles during liver injury and repair. *J. Clin. Invest.* 115:56–65.
48. Ginhoux, F., F. Tacke, V. Angeli, M. Bogunovic, M. Loubeau, X.M. Dai, E.R. Stanley, G.J. Randolph, and M. Merad. 2006. Langerhans cells arise from monocytes in vivo. *Nat. Immunol.* 7:265–273.
49. De Rossi, M., P. Bernasconi, F. Baggi, R. de Waal Malefyt, and R. Mantegazza. 2000. Cytokines and chemokines are both expressed by human myoblasts: possible relevance for the immune pathogenesis of muscle inflammation. *Int. Immunol.* 12:1329–1335.
50. Hirata, A., S. Masuda, T. Tamura, K. Kai, K. Ojima, A. Fukase, K. Motoyoshi, K. Kamakura, Y. Miyagoe-Suzuki, and S. Takeda. 2003. Expression profiling of cytokines and related genes in regenerating skeletal muscle after cardiotoxin injection: a role for osteopontin. *Am. J. Pathol.* 163:203–215.

51. Zhao, P., S. Iezzi, E. Carver, D. Dressman, T. Gridley, V. Sartorelli, and E.P. Hoffman. 2002. Slug is a novel downstream target of MyoD. Temporal profiling in muscle regeneration. *J. Biol. Chem.* 277:30091–30101.
52. Lumeng, C.N., J.L. Bodzin, and A.R. Saltiel. 2007. Obesity induces a phenotypic switch in adipose tissue macrophage polarization. *J. Clin. Invest.* 117:175–184.
53. Fujiwara, N., and K. Kobayashi. 2005. Macrophages in inflammation. *Curr. Drug Targets Inflamm. Allergy.* 4:281–286.
54. Serhan, C.N., and J. Savill. 2005. Resolution of inflammation: the beginning programs the end. *Nat. Immunol.* 6:1191–1197.
55. Hirt, U.A., and M. Leist. 2003. Rapid, noninflammatory and PS-dependent phagocytic clearance of necrotic cells. *Cell Death Differ.* 10:1156–1164.
56. Celada, A., and R.A. Maki. 1992. Transforming growth factor-beta enhances the M-CSF and GM-CSF-stimulated proliferation of macrophages. *J. Immunol.* 148:1102–1105.
57. Valledor, A.F., M. Comalada, J. Xaus, and A. Celada. 2000. The differential time-course of extracellular-regulated kinase activity correlates with the macrophage response toward proliferation or activation. *J. Biol. Chem.* 275:7403–7409.
58. Xaus, J., M. Cardo, A.F. Valledor, C. Soler, J. Lloberas, and A. Celada. 1999. Interferon gamma induces the expression of p21waf-1 and arrests macrophage cell cycle, preventing induction of apoptosis. *Immunity.* 11:103–113.
59. Gordon, S. 1999. Macrophage-restricted molecules: role in differentiation and activation. *Immunol. Lett.* 65:5–8.
60. Gonzalez-Juarrero, M., and I.M. Orme. 2001. Characterization of murine lung dendritic cells infected with *Mycobacterium tuberculosis*. *Infect. Immun.* 69:1127–1133.
61. Liu, G., X.P. Xia, S.L. Gong, and Y. Zhao. 2006. The macrophage heterogeneity: difference between mouse peritoneal exudate and splenic F4/80+ macrophages. *J. Cell. Physiol.* 209:341–352.
62. Carenini, S., M. Maurer, A. Werner, H. Blazyca, K.V. Toyka, C.D. Schmid, G. Raivich, and R. Martini. 2001. The role of macrophages in demyelinating peripheral nervous system of mice heterozygously deficient in p0. *J. Cell Biol.* 152:301–308.
63. Wehling, M., M.J. Spencer, and J.G. Tidball. 2001. A nitric oxide synthase transgene ameliorates muscular dystrophy in mdx mice. *J. Cell Biol.* 155:123–131.
64. Luk, H.W., L.J. Noble, and Z. Werb. 2003. Macrophages contribute to the maintenance of stable regenerating neurites following peripheral nerve injury. *J. Neurosci. Res.* 73:644–658.
65. Pull, S.L., J.M. Doherty, J.C. Mills, J.I. Gordon, and T.S. Stappenbeck. 2004. Activated macrophages are an adaptive element of the colonic epithelial progenitor niche necessary for regenerative responses to injury. *Proc. Natl. Acad. Sci. USA.* 102:99–104.
66. Rai, R.M., S. Loffreda, C.L. Karp, S.Q. Yang, H.Z. Lin, and A.M. Diehl. 1997. Kupffer cell depletion abolishes induction of interleukin-10 and permits sustained overexpression of tumor necrosis factor alpha messenger RNA in the regenerating rat liver. *Hepatology.* 25:889–895.
67. Rapalino, O., O. Lazarov-Spiegler, E. Agranov, G.J. Velan, E. Yoles, M. Fraidakis, A. Solomon, R. Gepstein, A. Katz, M. Belkin, et al. 1998. Implantation of stimulated homologous macrophages results in partial recovery of paraplegic rats. *Nat. Med.* 4:814–821.
68. Sadahira, Y., and M. Mori. 1999. Role of the macrophage in erythropoiesis. *Pathol. Int.* 49:841–848.
69. Diemel, L.T., S.J. Jackson, and M.L. Cuzner. 2003. Role for TGF-beta1, FGF-2 and PDGF-AA in a myelination of CNS aggregate cultures enriched with macrophages. *J. Neurosci. Res.* 74:858–867.
70. Butovsky, O., Y. Ziv, A. Schwartz, G. Landa, A.E. Talpalar, S. Pluchino, G. Martino, and M. Schwartz. 2006. Microglia activated by IL-4 or IFN-gamma differentially induce neurogenesis and oligodendrogenesis from adult stem/progenitor cells. *Mol. Cell. Neurosci.* 31:149–160.
71. Langen, R.C., J.L. Van Der Velden, A.M. Schols, M.C. Kelders, E.F. Wouters, and Y.M. Janssen-Heininger. 2004. Tumor necrosis factor-alpha inhibits myogenic differentiation through MyoD protein destabilization. *FASEB J.* 18:227–237.
72. Li, Y.P. 2003. TNF-alpha is a mitogen in skeletal muscle. *Am. J. Physiol. Cell Physiol.* 285:C370–C376.
73. Broussard, S.R., R.H. McCusker, J.E. Novakofski, K. Strle, W.H. Shen, R.W. Johnson, R. Dantzer, and K.W. Kelley. 2004. IL-1beta impairs insulin-like growth factor i-induced differentiation and downstream activation signals of the insulin-like growth factor i receptor in myoblasts. *J. Immunol.* 172:7713–7720.
74. Lefaucheur, J.P., and A. Sebille. 1995. Muscle regeneration following injury can be modified in vivo by immune neutralization of basic fibroblast growth factor, transforming growth factor beta 1 or insulin-like growth factor I. *J. Neuroimmunol.* 57:85–91.
75. Bondesen, B.A., S.T. Mills, and G.K. Pavlath. 2006. The COX-2 pathway regulates growth of atrophied muscle via multiple mechanisms. *Am. J. Physiol. Cell Physiol.* 290:C1651–C1659.
76. Horsley, V., and G.K. Pavlath. 2003. Prostaglandin F2α stimulates growth of skeletal muscle cells via an NFATC2-dependent pathway. *J. Cell Biol.* 161:111–118.
77. Shen, W., V. Prisk, Y. Li, W. Foster, and J. Huard. 2006. Inhibited skeletal muscle healing in cyclooxygenase-2 gene-deficient mice: the role of PGE2 and PGF2alpha. *J. Appl. Physiol.* 101:1215–1221.
78. Tidball, J.G., and M. Wehling-Henricks. 2007. Macrophages promote muscle membrane repair and muscle fiber growth and regeneration during modified muscle loading in vivo. *J. Physiol.* 578:327–336.
79. van Rooijen, N., and A. Sanders. 1994. Liposome mediated depletion of macrophages: mechanism of action, preparation of liposomes and applications. *J. Immunol. Methods.* 174:83–93.